JOURNAL OF MATERIALS SCIENCE 30 (1995) 47–52

Inhomogeneity of the crystallographic texture in a hot-rolled austenitic stainless steel

D. RAABE
Institut für Metallkunde und Metallphysik, RWTH Aachen, Kopernikusstr. 14, 52056 Aachen, Germany

The profile of the crystallographic texture through the thickness of a hot-rolled austenitic stainless steel containing 18% Cr and 8.5% Ni was examined. Although the hot-rolled strip generally revealed a weak orientation distribution, a considerable texture gradient occurred between the central layers and the surface layers. In the centre of the sheet a cold-rolling type of texture, that is, a β-fibre accompanied by a cubic orientation, was detected. It was assumed that this texture was formed during the last hot-rolling passes. Close to the surface, however, a shear texture consisting of a γ-fibre, a $\{0\,0\,1\}\langle 1\,1\,0\rangle$ and a $\{1\,1\,2\}\langle 1\,1\,0\rangle$ component was revealed. The absence of a maximum of the shear texture at $s = 0.7$–0.8 will be discussed in terms of the recrystallization.

1. Introduction

Flat products of austenitic and ferritic stainless steels are often industrially manufactured by continuous casting, hot rolling, subsequent cold rolling and final recrystallization. Whereas these processing steps usually lead to a homogeneous profile of the texture and the microstructure through the sheet thickness, the hot-rolling procedure is often the source of strong inhomogeneities [1–7].

Ferritic stainless steels with a chromium content of 11–17% [1–3] and transformer steels with a silicium content of 3.4% [3, 4] undergo a small volume fraction of the austenitic–ferritic phase transformation during cooling after hot rolling. This leads to the evolution of a strong through-thickness profile of the texture characterized by a cold-rolling type of orientation distribution in the central layers and a strong shear texture close to the sheet surface. It has previously been found [1–4] that the through-thickness course of this texture inhomogeneity corresponds to the profile of the externally imposed macroscopic shear [5–7]. If no phase transformation takes place, this texture profile is preserved since it is not randomized during cooling after the hot rolling. If low-carbon steels (which usually reveal a very weak through-texture inhomogeneity after hot rolling due to their high amount of phase transformation during subsequent cooling) are deformed thermomechanically–that is, if the final rolling steps are carried out mainly in the two-phase region–a strong inhomogeneity of the texture through the sheet thickness also results from the hot rolling [8]. If, however, hot rolling of face-centred cubic (f.c.c.) steels is executed in the austenitic-phase region, no phase transition can occur during the cooling, and the evolution of the texture gradient through the thickness of the sheet is likely to be similar to that in ferritic stainless steels. As was thoroughly proven for body-centred cubic (b.c.c) stainless steels [1, 2] and for transformer steels [3, 4], these initial texture inhomogeneities are passed on in the subsequent processing steps and they even affected the properties of the final products.

While the microstructure and texture of cold-rolled and recrystallized austenitic stainless steels have been subject to detailed investigations in the past [9–11], the inhomogeneity of the initial hot band has not yet been described in the literature. In the present work, therefore, the microstructure and the crystallographic texture of a hot-rolled austenitic alloy with a Chromium content of 18 wt % and a nickel content of 8.5 wt % was investigated and compared to findings of other stainless steels. For this purpose, the microstructure and texture was inspected through the sheet thickness of the hot band with a high local resolution.

2. Experimental procedure and the determination of the crystallographic textures

The hot-rolling process was industrially carried out after continuous casting and slab reheating in a conventional hot-strip mill. The band was unidirectionally rolled, in seven passes, to a thickness of 2.2 mm. The starting temperature was between 1420 and 1470 K during the first hot-rolling pass and it was in the range 1050–1200 K during the last pass.

Since the texture and the microstructure of stainless steels is often inhomogeneous through the thickness [1–3], the samples were inspected in various layers. In

order to describe each inspected layer the parameter $s = a/(\frac{1}{2}d)$ was defined, where a, was the distance from the centre layer and d was the thickness of the sheet; that is, the surface layer has the value $s = 1$ and the centre layer has the value $s = 0$. The textures of the hot-rolled strip were inspected in steps of $\Delta s = 0.1$.

To remove a surface layer of 20×10^{-6} m, (to remove disturbing grinding effects before the texture measurements) the samples were etched in a solution of 100 ml H_2O, 100 ml HCl and 30 ml HNO_3 at the ambient temperature.

The crystallographic textures were quantitatively examined by measuring four incomplete pole figures {1 1 1}, {2 0 0}, {2 2 0} and {1 1 3} by use of Mo$K_{\alpha 1}$ radiation in the back-reflection mode [12]. From the pole figures which are two-dimensional projections of the texture, the three-dimensional orientation distribution function (ODF) was computed by use of a series-expansion method [13]. For cubic crystal symmetry and orthorhombic sample symmetry which is set up by the rolling, normal and transverse directions (RD, ND and TD respectively), an orientation can be represented by the three Euler angles φ_1, ϕ and φ_2. For clarity, an orientation is often presented in terms of the Miller indices $\{hkl\}$ $\langle$u v w$\rangle$, where $\{hkl\}$ describes the crystallographic plane which is parallel to the sheet surface and $\langle uvw\rangle$ describes the crystal direction that is parallel to the RD.

Since austenitic steels tend to develop characteristic fibre textures during rolling deformation [9–11, 14], it is convenient to depict the ODFs as iso-intensity diagrams in φ_2-sections through the Euler space. Fig. 1 gives the most relevant texture components where:

the α-fibre has $\langle 1\,1\,0\rangle \parallel$ ND, and its main orientations are $\{0\,1\,1\}\langle 1\,0\,0\rangle$, $\{0\,1\,1\}\langle 2\,1\,1\rangle$, $\{0\,1\,1\}\langle 1\,1\,1\rangle$ and $\{0\,1\,1\}\langle 0\,1\,1\rangle$,

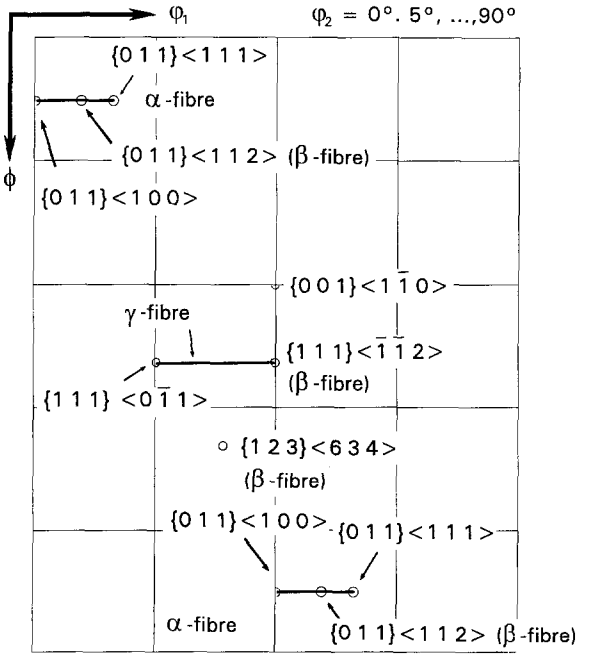

Figure 1 Relevant texture components in φ_2-sections through the Euler space.

the γ-fibre has $\{1\,1\,1\} \parallel$ ND, and its main orientations are $\{1\,1\,1\}\langle 1\,1\,0\rangle$, $\{1\,1\,1\}\langle 1\,1\,2\rangle$,

the β-fibre has a less-symmetric-texture fibre containing the orientations $\{1\,1\,2\}\langle 1\,1\,1\rangle$(C), $\{1\,2\,3\}\langle 6\,3\,4\rangle$ (S) and $\{0\,1\,1\}\langle 2\,1\,1\rangle$ (B).

3. Experimental results

As can be seen in the longitudinal section in Fig. 2 the hot-rolled material had a homogeneous microstructure through the thickness of the sheet. Many twin boundaries occur in all the layers. The grain size was about 12 μm in all the layers, since the twin boundaries were treated as usual large-angle grain boundaries. The microstructure is more homogeneous than that of hot-rolled ferritic stainless steels [1–3].

The hot band had an inhomogeneous texture profile through the thickness of the sheet. Close to the centre layer (that is, at $s = 0$ and $s = 0.1$) the orientation distribution was characterized by a weak β-fibre with a maximum at $\{0\,1\,1\}\langle 2\,1\,1\rangle$ (Fig. 3a and b). A Continuously developed α-fibre as in cold-rolled f.c.c. materials does not appear (Fig. 4). A second relevant property of the texture at $s = 0$ and $s = 0.1$ is the appearance of the cubic component $\{1\,0\,0\}\langle 1\,0\,0\rangle$ (Fig. 3a and b and Fig. 5). In the layers $s = 0.2$ and $s = 0.3$ the orientations mentioned above had completely decreased and a nearly random orientation distribution was revealed, (Fig. 3c and d). In the layers

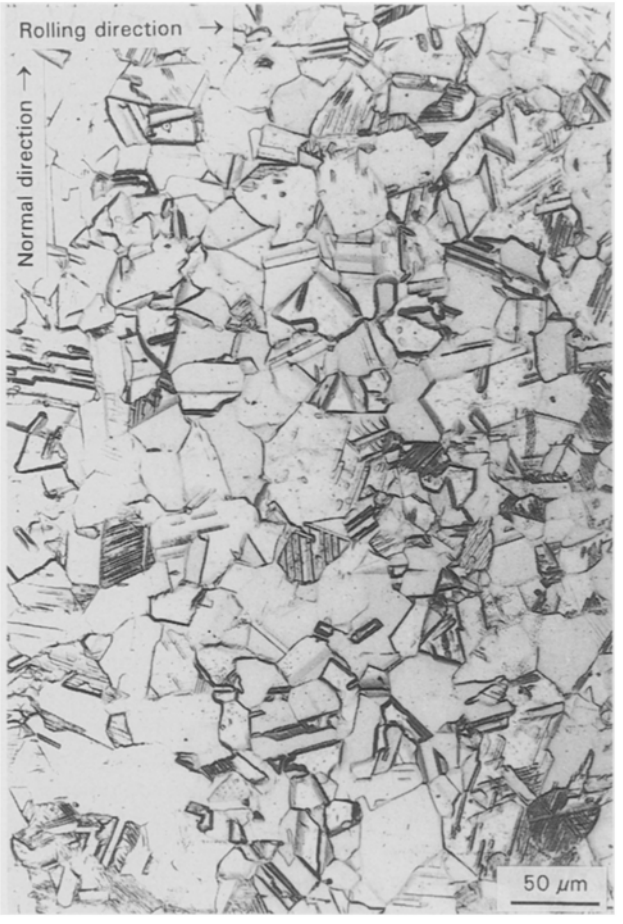

Figure 2 A Longitudinal section of the austenitic hot band.

$s = 0.4 - 0.6$ a texture transition took place, Fig. 3e–g. First, a weak $\{0\,0\,1\}\langle 1\,1\,0\rangle$ component (Fig. 5), secondly, a γ-fibre (Fig. 6) and, thirdly, a strong $\{1\,1\,2\}\langle 1\,1\,0\rangle$ orientation, which corresponds to the 30° about TD rotated f.c.c. rolling component $\{1\,1\,0\}\langle 1\,1\,2\rangle$, (Fig. 3g) were generated. In the subsurface layers (that is, at $s = 0.7$ and $s = 0.8$) the orientation distribution became considerably weaker (Fig. 3h and i). At the surface, $s = 0.9$ and $s = 1$, a similar texture developed to that in the layer $s = 0.6$ (Fig. 3j and k).

In order to illustrate the gradient of the orientation distribution through the thickness of the hot-rolled sheet, the three dominant texture components (namely, $\{0\,0\,1\}\langle 1\,1\,0\rangle$, $\{1\,1\,2\}\langle 1\,1\,0\rangle$) and the maximum close to $\{1\,1\,1\}\langle 1\,1\,0\rangle$ on the γ-fibre of Fig. 6, were applied as indicators in Fig. 7. The orientation density of all three of the characteristic components

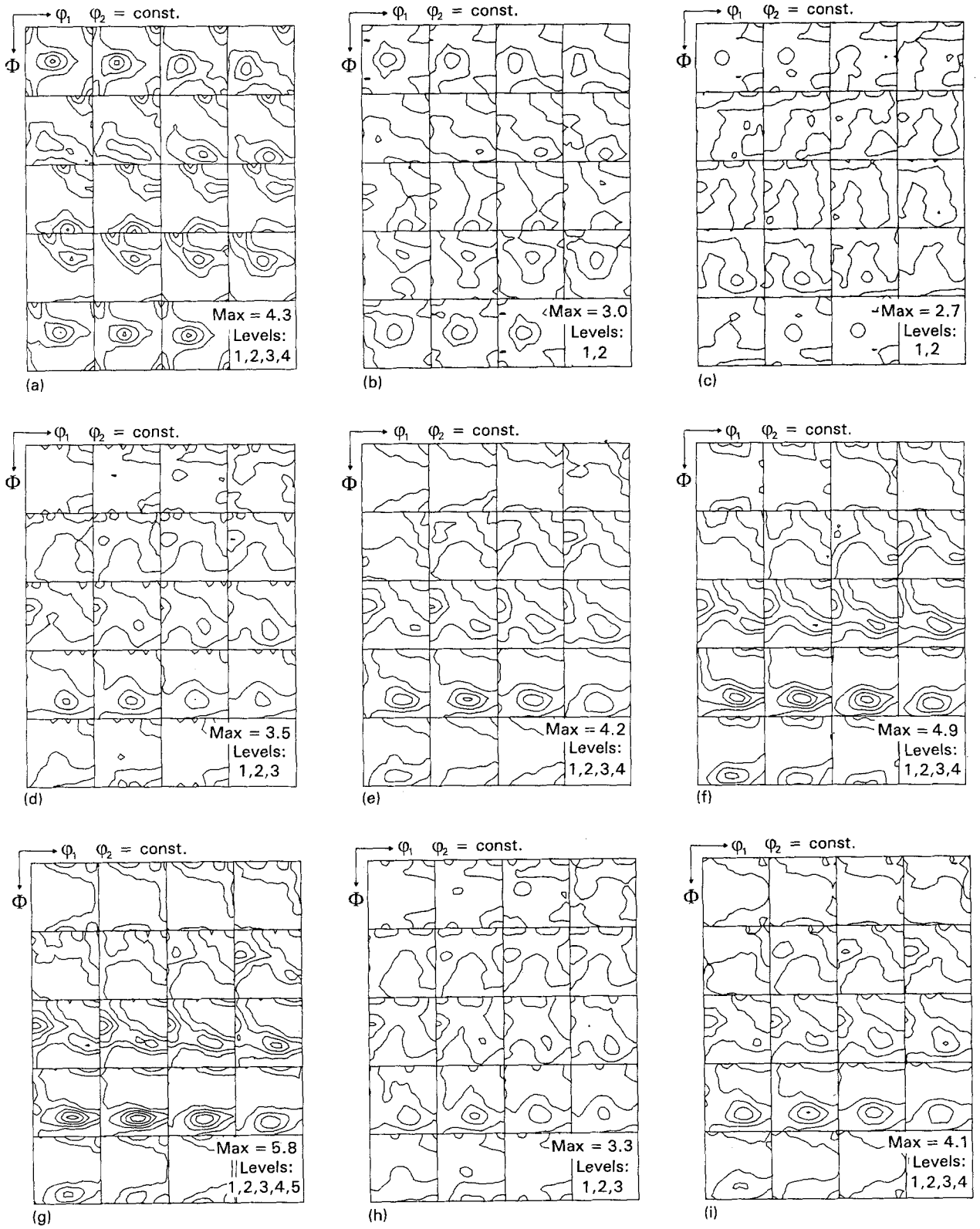

Figure 3 ODFs through the thickness of the austenitic hot band: (a) $s = 0$, centre layer, (b) $s = 0.1$, (c) $s = 0.2$, (d) $s = 0.3$, (e) $s = 0.4$, (f) $s = 0.5$, (g) $s = 0.6$, (h) $s = 0.7$, (i) $s = 0.8$, (j) $s = 0.9$ and (k) $s = 1$, surface layer.

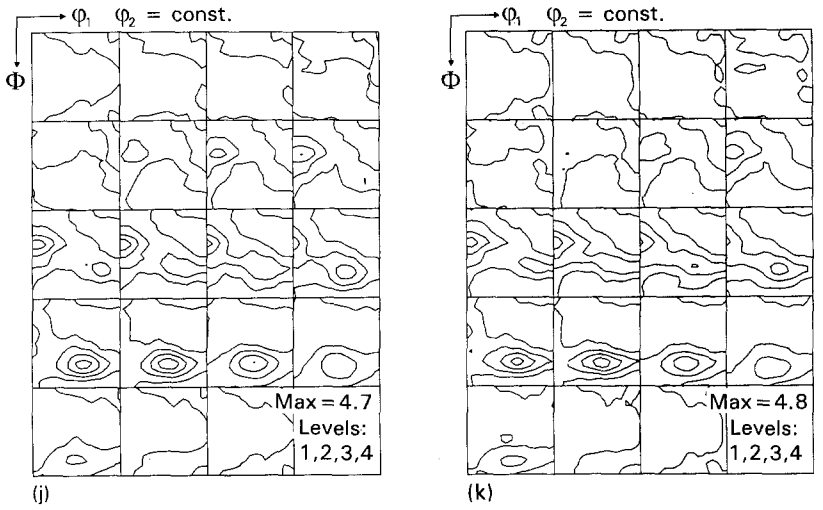

Figure 3 (continued)

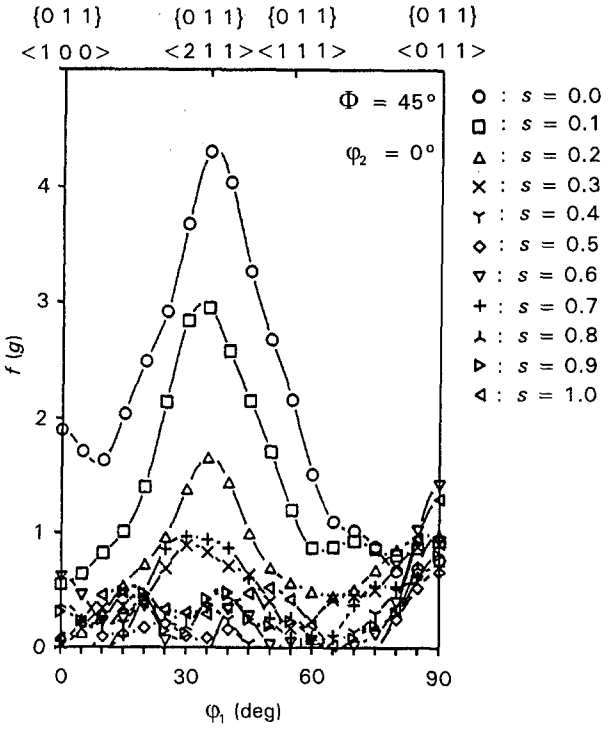

Figure 4 The through-thickness texture profile for an α-fibre.

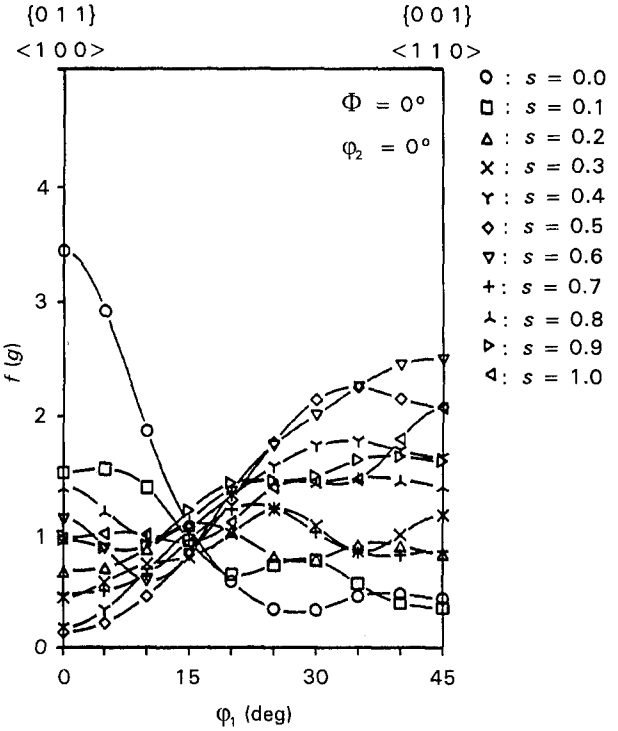

Figure 5 The through-thickness texture profile for a cubic ND-rotation fibre.

had an identical course through the thickness of the sheet. Close to the centre layers, all three of the orientations were very weak and they continuously increased up to the layer $s = 0.6$; while between $s = 0.6$ and $s = 0.9$ the texture decreased, and at the surface (that is, at $s = 1$) the texture increased.

4. Discussion

The main feature of the hot-band texture is the occurrence and the course of the through-thickness inhomogeneity which is characterized by a weak β-fibre accompanied by a cubic orientation in the central layers (Fig. 3a and b) and also by the occurrence of two separate through-thickness maxima of a γ-fibre, the $\{001\}\langle110\rangle$ and the $\{112\}\langle110\rangle$ component close to the surface at $s = 0.6$ (Figs 3g and 7) and at $s = 1$ (Figs 3k and 7).

In accordance with numerous experimental results by Goodman and Hu [9], Donadille *et al.* [10] and Rickert and Salsgiver [11] for austenitic stainless steels and with Taylor-type simulations by Hirsch and Lücke [14] and Fortunier and Hirsch [15] for f.c.c. materials, the observed β-fibre at $s = 0$ and $s = 0.1$ (Fig. 3a and b) is a typical texture which is generated during the plane-strain rolling deformation of f.c.c. polycrystals at ambient temperatures, although in the present case the observed maximum of the orientation

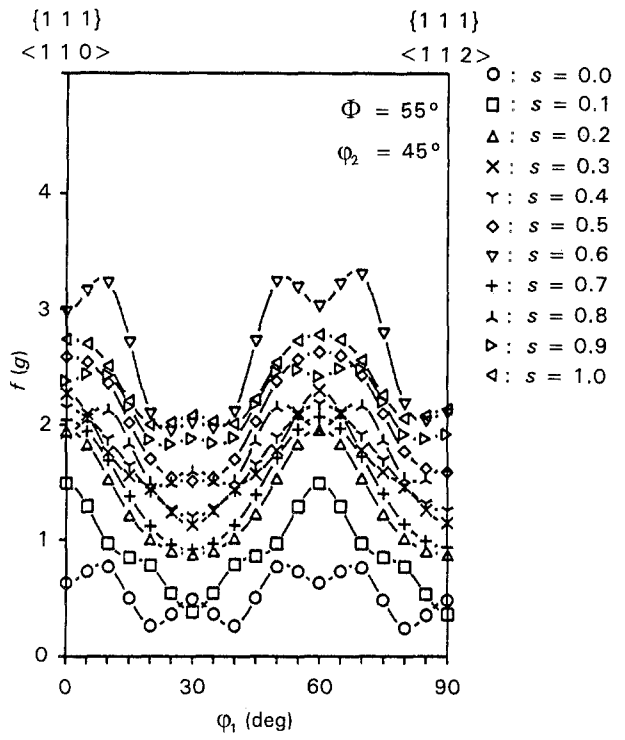

Figure 6 The through-thickness texture profile, for a γ-fibre.

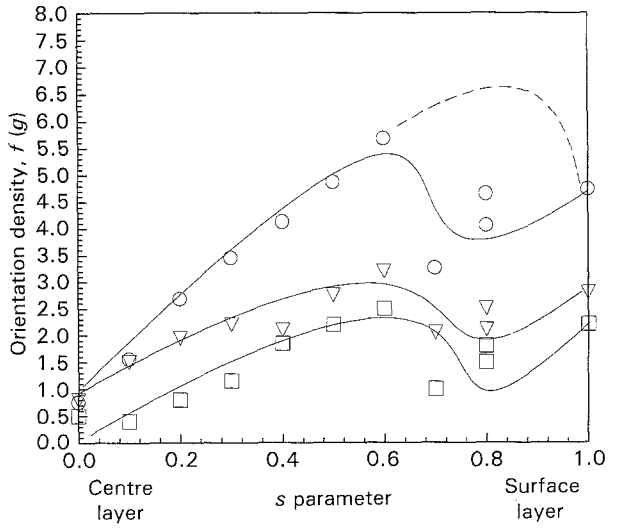

Figure 7 The through-thickness texture profile, indicated by the course of the three main texture components: (□) {0 0 1}⟨1 1 0⟩, (○) {1 1 2}⟨1 1 0⟩, and (▽) the γ-fibre maximum.

density was considerably lower than it was after cold rolling. Since complete recrystallization during or after hot rolling would have removed the rolling texture which was detected in the central layers, this result suggests, to a first approximation, that during hot rolling a high volume fraction of material has merely undergone recovery. This assumption, however, contradicts the following four further findings. First, the microstructure (Fig. 2) had fairly equiaxed, rather than an elongated, recovered grain morphology. Secondly the stacking-fault energy (SFE) of the inspected austenitic stainless steels was very low, namely, 21×10^{-3} J m^{-2} [16], so that the corresponding normalized value (that is, the SFE divided by the Burgers vector and the shear modulus) was equal to 0.68×10^{-3}, which has a value similar to 70/30 brass alloy. This fact suggests that a tendency for recrystallization instead for recovery should be expected. Thirdly the low absolute orientation density in all the layers indicates that, at least during the first hot-rolling passes, recrystallization must have taken place since steady recovery would have led to a much higher texture maximum. Fourthly, the starting temperature of about 1420–1470 K led to a homologous temperature, T/T_m, of about 0.8 which also favoured recrystallization rather than recovery.

It is thus more likely that recrystallization restored the microstructure during the first hot-rolling passes and that the weak β-fibre texture which was detected was developed during the last rolling passes, where the band temperature had dropped. This explanation would imply a low recrystallization tendency, with a low stored dislocation energy imposed by the last rolling passes.

The second relevant feature of the central layer texture of the hot band is the occurrence of the cubic orientation (Figs 3a, b and 5). This component was also detected in the central layers of hot-rolled aluminium [17]. According to Le Hazif *et al.* [18] and Maurice and Driver [19] (who have carried out slip-line investigations on hot-worked aluminium), the cubic orientation is attributable to the activation of dislocation slip on {1 1 0}⟨1 1 0⟩ in addition to the conventional octahedral slip systems at homologous temperatures above 0.6. In accordance with the arguments above, and especially the much lower SFE of the austenite, it is, however, most likely that the observed cubic component resulted from recrystallization rather than from deformation.

The textures in the other layers showed the main differences in the orientation distribution at $s = 0$ and $s = 0.1$. In some layers a random texture occurred (Fig. 3c, d and h), while at $s = 0.6$ (Figs 3g and 7) and at $s = 1$ (Figs 3k and 7) a γ-fibre, accompanied by a {0 0 1}⟨1 1 0⟩ and {1 1 2}⟨1 1 0⟩ orientation, was discovered. All three texture components are known to occur in inhomogeneously hot-rolled aluminium and they are typical of the orientations generated by strong shear deformation [7, 20]. According to Mao [20], the {1 1 2}⟨1 1 0⟩ component results from the {0 1 1}⟨2 1 1⟩ orientation, which represents the strongest plane-strain rolling component in f.c.c. metals with a low SFE and which has been rotated 30° about the TD due to the rotation of the strain state [7]. A similar through-thickness profile of the corresponding shear orientations in b.c.c. materials has also been thoroughly investigated for hot-rolled ferritic stainless steels [1–3, 7] and for transformer steels [4]. In these works, however, the strongest shear component (and therefore the highest orientation densities of the shear texture components) occurred at $s = 07$–0.8, while in the austenitic hot band investigated in our study the maximum of the shear texture was locally split into one peak at $s = 0.6$ and into a second peak at $s = 1$. At $s = 0.7$–0.8, in contrast, a local minimum of the relevant texture components (which serve as indicators for shear deformation) can even be seen in

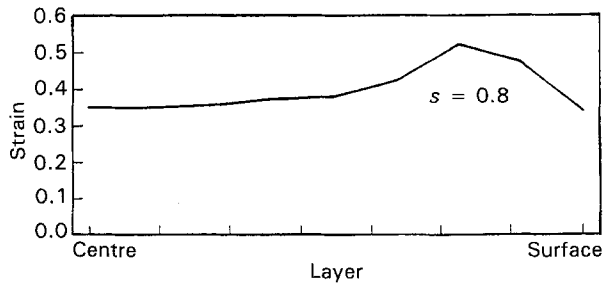

Figure 8 The simulated through-thickness profile of the von Mises equivalent shear, according to Beynon *et al.* [5].

(Fig. 7. Although the observed orientation densities are very weak, this effect clearly contradicts the experimentally detected profiles in [1–4, 7] and the calculated shear profiles submitted by Beynon *et al.* [5] and by McLaren and Sellars [6] for the industrial-hot-rolling of stainless steels (see Fig. 8).

In order to interpret the observed texture profile it is suggested that the expected maximum in the shear was indeed situated in the range $s = 0.7$–0.8, as predicted by the simulations in [5–7] and as schematically marked by the dashed line in Fig. 7. But since this implies a higher local deformation (that is, a higher stored dislocation energy) in these layers ($s = 0.7$–0.8) recrystallization could easily have taken place due to the low SFE of the austenite, leading to a randomization of the texture. The strong increase of the recrystallized volume fraction at $s = 0.7$–0.8 in the hot-rolled strip was predicted by McLaren and Sellars [6]. In contrast, the experimental findings in b.c.c. steels [1, 2, 17, 20], which had a maximum of the shear texture at $s = 0.7$–0.8, have to be attributed to the higher SFE, implying a higher tendency to recover, that is to preserve the shear texture.

The observed texture profile – which is thus mainly attributable to the through-thickness profile of the shear which is (in accordance with the simulations in [5–7] and the experiments in [1, 2, 17, 20]) assumed to occur during the last (or during the last two) hot-rolling passes – only weakly relates to the homogeneous microstructure through the sheet thickness.

5. Conclusion

The through-thickness profile of the microstructure and texture in a hot-rolled austenitic stainless steel with 18% Cr and 8.5% Ni was investigated. The hot band had a weak orientation distribution with a texture gradient between the centre and the surface layers. In the centre of the sheet a cold-rolling type texture, that is, a β-fibre with a cubic orientation was detected; this was not randomized by recrystallization. It was assumed, therefore, that this texture was essentially formed during the last hot-rolling passes. Close to the surface, a shear texture consisting of a γ-fibre, a $\{0\,0\,1\}\langle 1\,1\,0\rangle$ and a $\{1\,1\,2\}\langle 1\,1\,0\rangle$ component were detected; this corresponds to similar findings in hot-rolled aluminium. The absence of the maximum of the shear texture at $s = 0.7 - 0.8$ was explainable by recrystallization.

Acknowledgements

The author gratefully acknowledges the kind support from the Krupp-Hoesch Stahl AG, especially from Dr M. Hölscher.

References

1. D. RAABE, and K. LÜCKE, *Mater. Sci. Technol.* **9** (1993) 302.
2. M. HÖLSCHER, D. RAABE and K. LÜCKE, *Steel Research* **62** (1991) 567.
3. D. RAABE and K. LÜCKE, *Scripta Metall. Mater.* **26** (1992) 1221.
4. L. SEIDEL, M. HÖLSCHER and K. LÜCKE, *Textures Microstruc.* **11** (1989) 171.
5. J. H. BEYNON, P. R. BROWN, S. I. MIZBAN, A. R. S. PONTER and C. M. SELLARS, in "Computational Techniques for Predicting Material Processing Defects" edtied by M. Predeleanu (Elsevier, Amsterdam, 1987) pp. 19–28.
6. A. J. MCLAREN and C. M. SELLARS, *Mater. Sci. Technol.* **8** (1992) 1090.
7. M. HÖLSCHER, D. RAABE and K. LÜCKE, *Acta Metall. Mater.* in press.
8. C. DÄRMANN and B. ENGL, *Steel Research* **62** (1991) 576.
9. S. R. GOODMAN and H. HU, *Trans. AIME* **230** (1964) 1413.
10. C. DONADILLE, R. VALLE, P. DERVIN and R. PENELLE, *Acta Metall. Mater.* **37** (1989) 1547.
11. T. J. RICKERT and J. A. SALSGIVER, Proceedings of the 10th International Conference on Textures of Materials. ICOTOM 10 (Clausthal, 1993) in press.
12. L. G. SCHULZ, *J. Appl. Phys.* **20** (1949) 1030.
13. H. J. BUNGE, "Texture Analysis in Materials Science", (Butter-worths, London, 1982).
14. J. HIRSCH and K. LÜCKE, *Acta Metall. Mater.* **36** (1988) 2863.
15. R. FORTUNIER and J. HIRSCH in "Theoretical Methods of Texture Analysis" edited by H. J. Bunge, (Verlag Deutsche Gesellschaft fur Materialkunde Info. gesellsch., 1987) p. 231.
16. R. E. SCHRAMM and R. P. REED, *Metall. Trans. A* **6** (1975) 1345.
17. J. HIRSCH in "Hot Deformation of Aluminium Alloys" edited by G. T. Langdon, M. D. Merchant, J. G. Morris and M. A. Zaidi (Transaction of The Metals Society, 1991) p. 379.
18. R. LE HAZIF, P. DORIZZI and J. P. POIRIER, *Acta Metall. et Mater.* **21** (1973) 903.
19. CL. MAURICE and J. H. DRIVER, *ibid.* **41** (1993) 1653.
20. W. MAO, Doctoral thesis, Rheinisch Westfälische Technische Hochschule, Aachen (1988) III-11 and III-28.

Received 2 February
and accepted 27 May 1994